

ORIGINAL ARTICLE

Noonan syndrome-associated biallelic *LZTR1* mutations cause cardiac hypertrophy and vascular malformations in zebrafish

Yu Nakagama^{1,2}  | Norihiko Takeda³ | Seishi Ogawa⁴ | Hiroyuki Takeda⁵ | Yoshiyuki Furutani⁶ | Toshio Nakanishi⁶ | Tatsuyuki Sato³ | Yoichiro Hirata¹ | Akira Oka¹ | Ryo Inuzuka¹

¹Department of Pediatrics, Graduate School of Medicine, The University of Tokyo, Tokyo, Japan

²Department of Parasitology, Graduate School of Medicine, Osaka City University, Osaka, Japan

³Department of Cardiovascular Medicine, Graduate School of Medicine, The University of Tokyo, Tokyo, Japan

⁴Department of Pathology and Tumor Biology, Graduate School of Medicine, Kyoto University, Kyoto, Japan

⁵Department of Biological Sciences, Graduate School of Science, The University of Tokyo, Tokyo, Japan

⁶Department of Pediatric Cardiology and Adult Congenital Cardiology, Tokyo Women's Medical University, Tokyo, Japan

Correspondence

Ryo Inuzuka, Department of Pediatrics, Graduate School of Medicine, The University of Tokyo, 7-3-1 Hongo, Bunkyo-ku, Tokyo 113-8655, Japan.
Email: inuzukar-ky@umin.ac.jp

Funding information

Japan Society for the Promotion of Science, Grant/Award Number: JP17J09192; Morinaga Foundation for Health & Nutrition; Miyata Foundation

Abstract

Background: Variants in the *LZTR1* (*leucine-zipper-like transcription regulator 1*) gene (OMIM #600574) have been reported in recessive Noonan syndrome patients. In vivo evidence from animal models to support its causative role is lacking.

Methods: By CRISPR-Cas9 genome editing, we generated *lztr1*-mutated zebrafish (*Danio rerio*). Analyses of histopathology and downstream signaling were performed to investigate the pathogenesis of cardiac and extracardiac abnormalities in Noonan syndrome.

Results: A frameshift deletion allele was created in the zebrafish *lztr1*. Crosses of heterozygotes obtained homozygous *lztr1* null mutants that modeled *LZTR1* loss-of-function. Histological analyses of the model revealed ventricular hypertrophy, the deleterious signature of Noonan syndrome-associated cardiomyopathy. Further, assessment for extracardiac abnormalities documented multiple vascular malformations, resembling human vascular pathology caused by RAS/MAPK activation. Due to spatiotemporal regulation of *LZTR1*, its downstream function was not fully elucidated from western blots of adult tissue.

Conclusion: Our novel zebrafish model phenocopied human recessive Noonan syndrome and supported the loss-of-function mechanism of disease-causing *LZTR1* variants. The discovery of vascular malformations in mutants calls for the clinical follow-up of patients to monitor for its emergence. The model will serve as a novel platform for investigating the pathophysiology linking RAS/MAPK signaling to cardiac and vascular pathology.

KEYWORDS

hypertrophic cardiomyopathy, *LZTR1*, Noonan syndrome, RAS/MAPK syndrome, vascular malformation

1 | INTRODUCTION

The genetic spectrum of Noonan syndrome (NS), a multisystem disorder with cardiac involvement, is highly heterogeneous

and still expanding. Eighty percent of the patients carry dominant mutations in either the *PTPN11*, *KRAS*, *SOS1*, *SOS2*, *RAF1*, *NRAS*, *BRAF*, or *RIT1*, all of which are members of the RAS/MAPK signaling cascade (Aoki, Niihori, Inoue, &

This is an open access article under the terms of the Creative Commons Attribution-NonCommercial-NoDerivs License, which permits use and distribution in any medium, provided the original work is properly cited, the use is non-commercial and no modifications or adaptations are made.

© 2019 The Authors. *Molecular Genetics & Genomic Medicine* published by Wiley Periodicals, Inc.

Matsubara, 2016). Recently, recessive variants in the *LZTR1* (*leucine-zipper-like transcription regulator 1*) gene (OMIM #600574) were identified from genetic analyses of NS patients who had tested negative for known RAS/MAPK gene mutations (Johnston et al., 2018; Nakaguma, Jorge, & Arnhold, 2019; Umeki et al., 2018). *LZTR1* is now emerging as a novel causative gene of NS pathophysiology. To date, however, in vivo evidence from animal models is lacking to further support the role of biallelic *LZTR1* variants in causing autosomal-recessive NS. The main aim of the study here was to, by way of efficient genome editing in zebrafish (*Danio rerio*), add to the evidence that functional loss of *LZTR1* directly leads to developing the hallmark histopathological features of NS.

2 | MATERIALS & METHODS

2.1 | Ethical compliance

Analyses involving human participants were conducted in accordance with the principles of the Declaration of Helsinki. The work was approved by the institutional ethics committee (#G3565). Written consent was obtained from all participants. Experimental procedures and animal care complied with the standards of animal ethics committee of The University of Tokyo.

2.2 | Exome sequencing and filtering of putative pathogenic variants

Exome capture libraries were constructed from genomic DNA of family members using SureSelect Human All Exon (50 Mb) V4 (Agilent). Enriched exome libraries were sequenced with the HiSeq 2000 (Illumina) platform. Variants were filtered according to allele frequency (below 0.001), in silico predictions (Polyphen2, SIFT), and familial segregation assuming autosomal-recessive inheritance.

2.3 | Generation of *lztr1* mutant zebrafish

Experiments were performed as described previously (Jao, Wente, & Chen, 2013). Oligonucleotides designed to target the zebrafish *lztr1* exon 2, “gRNA F” (5'-TTGTGGCATAACAGGGATGCC-3') and “gRNA R” (5'-GGCATCCCTGTATGCCACAA-3'), were cloned into a guide RNA expression vector. The mixture of guide RNA and Cas9 RNA was introduced into the one-cell stage embryos obtained from natural crosses of wild-type zebrafish of the AB background. F0 zebrafish were screened for random insertion/deletion mutations by PCR amplification of the targeted genomic region followed by

polyacrylamide gel electrophoresis-based genotyping (Zhu et al., 2014); genotyping primers used were “*lztr1* ex2 F” (5'-CTAACCACTGAGCCACCGTT-3') and “*lztr1* ex2 R” (5'-CTCACCCATTGTCTCCTCCA-3'). A chimeric F0 mutant harboring a frameshift, 7-bp deletion germline allele was identified and backcrossed to wild-type fish to obtain F1 heterozygotes (*lztr1*^{del/+}). F1 heterozygotes were crossed to generate F2 homozygous mutants (*lztr1*^{del/del}). Genotyping the *lztr1* mutant allele was done according to the emergence of a new BslI (New England Biolabs) digestion site (55°C incubation for 2 hr).

2.4 | RNA analysis

RNA extraction from zebrafish was performed using NucleoSpin RNA (Macherey-Nagel). cDNA was synthesized using ReverTra Ace Master Mix (Toyobo). Primers flanking the CRISPR-targeted *lztr1* exon (5'-TAACACTCAACTTCGGGCCT-3' and 5'-TAGTAAA CGCCGACACCAT-3') and primers located upstream of the *lztr1* deletion site (5'-TAACACTCAACTTCGGGCCT-3' and 5'-GGTATGCTTGCTACGCCTTG-3') were used for the sequencing and quantitative PCR analyses, respectively. Quantitative PCR was performed using THUNDERBIRD SYBR Mix (Toyobo) and analyzed with the LightCycler System (Roche Diagnostics). Values were normalized to *gapdh* expression (5'-GTGGAGTCTACTGGTGTCTTC-3' and 5'-GTGCAGGAGGCATTGCTTACA-3').

2.5 | Histological analysis

Hematoxylin-eosin and Masson's trichrome staining of formalin-fixed, paraffin-embedded adult zebrafish sections were performed following standard protocols. Stained sections were imaged on Leica DM2500 LED (Leica Microsystems). Quantification of cardiac hypertrophy was performed in Masson's trichrome heart sections using the ImageJ software (National Institutes of Health), as described previously (Abdul-Wajid, Demarest, & Yost, 2018). Original images were processed by splitting the color channels, subtracting the green from the red channel, and generating a novel composite image. A threshold for intensity was set to detect the cardiomyocytes demarcated in red by Masson's trichrome staining. Finally, the percentage of total ventricular area covered by myocardial tissue was determined.

2.6 | Western blot analysis

Heart tissue extracts from wild-type, *lztr1*^{del/+} and *lztr1*^{del/del} zebrafish, as well as protein extracts from transformed DH5 α

E. coli, were separated by 7.5% polyacrylamide gel electrophoresis and transferred onto polyvinylidene difluoride membranes. After blocking the membrane in 3% bovine serum albumin, 1× Tris-buffered saline with 0.1% Tween-20, the membrane was incubated with the primary antibodies and then with a horseradish peroxidase-conjugated secondary antibody. Detection was performed using ECL Prime (GE Healthcare). The following antibodies were used: anti-ERK 1/2 (1:1000, #4695, Cell Signaling Technology), anti-phospho-ERK 1/2 (1:1000, #4370, Cell Signaling Technology), anti-AKT (1:1000, #9272, Cell Signaling Technology), anti-phospho-AKT (1:1000, #4060, Cell Signaling Technology), anti-GST (1:2000, #27-4577-01, GE Healthcare), donkey anti-goat IgG-HRP (1:1000, #sc-2020, Santa Cruz Biotechnology), and mouse anti-rabbit IgG – HRP (1:1000, #sc-2357, Santa Cruz Biotechnology).

3 | RESULTS & DISCUSSION

Firstly, we identified a familial case of recessive inheritance heart disease, in which three of the four siblings were affected with pulmonary stenosis, ventricular septal defect, and biventricular cardiac hypertrophy, all of which are common cardiac manifestation of NS. Exome sequencing in search of disease-causing variants revealed a pair of compound heterozygous *LZTR1* variants (NM_006767.4:c.1605C > A [p.Tyr535Ter] [rs753347937] and NM_006767.4:c.2387T > C [p.Ile796Thr] [rs141672122]) that have never been associated with a disorder before but here co-segregated with

phenotype. According to the American College of Medical Genetics and Genomics consensus criteria (Richards et al., 2015), the former nonsense variant was evaluated as “pathogenic” and the latter as “likely pathogenic.” In line with the literature, our patients harbored a combination of one null and one putatively hypomorphic variant, further supporting the proposed loss-of-function mechanism of the disease (Johnston et al., 2018).

Next, in order to further support the causal relationship between recessive *LZTR1* variants and NS, we planned to model the disease in zebrafish using reverse genetics. We introduced random indel mutations by targeting the zebrafish *lztr1* exon 2 sequence (5'-TTGTGGCATAACAGGGATGCC-3'). We identified a frameshift 7-bp deletion germline allele leading to a premature termination codon (Figure 1a). Quantitative transcriptional analysis of the mutated allele found no evidence of nonsense-mediated decay acting as the primary mechanism of the loss-of-function (Figure 1b). Sequencing of transcripts from the mutated allele confirmed the frameshift and resultant premature termination at the mRNA level (Figure 1c). Since none of the commercially available antibodies had been verified for its use in detecting zebrafish endogenous *LZTR1* expression, we generated GST-tagged *LZTR1* and mutant *LZTR1*-expressing vectors and detected *LZTR1* expression using an anti-GST antibody. Western blot results showed that the frameshift 7-bp deletion indeed resulted in premature truncation of the *LZTR1* protein, confirming the null effect of the mutation (Figure 1b).

Further mating obtained F1 heterozygous *lztr1*^{del/+} and F2 homozygous *lztr1*^{del/del} mutants. F2 *lztr1*^{del/del} mutants were only obtained at a skewed genotype ratio from *lztr1*^{del/+} crosses

FIGURE 1 Modeling the Noonan syndrome-associated loss-of-function *LZTR1* mutations in zebrafish. (a) CRISPR/Cas9-based gene targeting induced a 7-bp frameshift deletion in exon 2 of the zebrafish (*Danio rerio*) *lztr1*. (b) Quantitative PCR analysis of the *lztr1* transcript showed comparable expression levels between different genotypes. Data are represented as the mean ± SD of technical triplicates from a representative experiment. (c) The effect of CRISPR induced 7-bp frameshift deletion on *lztr1* mRNA and protein sequence. (d) GST-tagged wild-type and mutated proteins were detected by western blot using anti-GST antibody. The 7-bp frameshift deletion resulted in premature truncation of the *LZTR1* protein

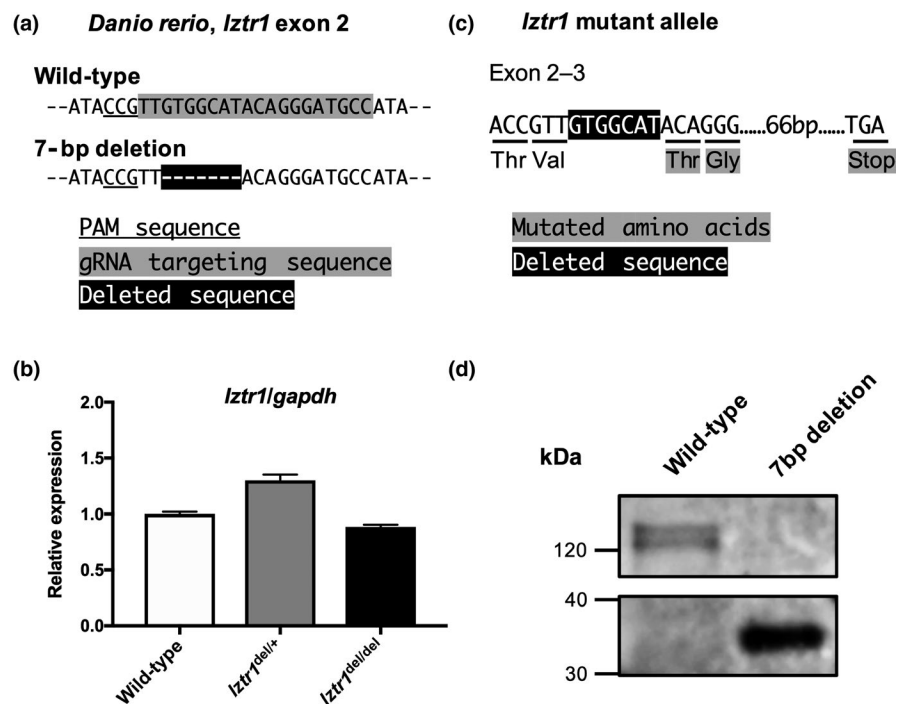


TABLE 1 Skewed progeny ratio obtained from $lztr1^{del/+} \times lztr1^{del/+}$ crosses

Progeny genotype	Frequency	%
$lztr1^{+/+}$	38	23.6
$lztr1^{del/+}$	110	68.3
$lztr1^{del/del}$	13	8.1
Total	161	

Note: The homozygous $lztr1^{del/del}$ mutants were obtained at a skewed genotype ratio from $lztr1^{del/+}$ crosses.

(13 of 161 progenies, 8.1%), suggesting a negative selection of the homozygotes related to some sort of core organ dysfunction (Table 1). We then performed histological analysis for description of the cardiac phenotype in $lztr1^{del/del}$ adult zebrafish. Longitudinal Masson's trichrome sections of 4–6 months old adult zebrafish showed marked cardiac hypertrophy in $lztr1^{del/del}$ fish (Figure 2a). Morphology of other cardiac structures, such as the bulbus arteriosus, did not differ significantly. As a quantitative index of cardiac hypertrophy, the percentage of ventricular area covered by myocardial tissue was measured (Abdul-Wajid et al., 2018). Percent coverage of ventricular area by cardiomyocytes was $45.1 \pm 3.1\%$ in control hearts and $55.9 \pm 2.1\%$ in $lztr1$ -ablated hearts (mean \pm SEM, $N = 3, 5, 5$ for wild-type, $lztr1^{del/+}$, $lztr1^{del/del}$, respectively), depicting significant ventricular hypertrophy in $lztr1^{del/del}$ fish (Figure 2b). Extracardiac anomalies were also assessed using hematoxylin-eosin–stained longitudinal sections (Figure 3a). Multiple vascular malformations were documented specifically in $lztr1^{del/del}$ homozygous mutants (8 out of 8 [100%] $lztr1^{del/del}$ fish analyzed), while none of the wild-type or $lztr1^{del/+}$ controls exhibited the phenotype (Table 2). These lesions observed in zebrafish resembled human vascular malformations caused by somatic activating variants in genes of the RAS/MAPK pathway: *KRAS*, *NRAS*, *BRAF*, and *MAP2K1* (Al-Olabi et al., 2018). Although patients with recessive Noonan syndrome have not yet been reported to manifest such vascular abnormalities, careful follow-up to monitor for its emergence is of clinical significance since these vascular malformations may lead to life-threatening bleeds, disfigurement, and/or pain.

Elucidation of the molecular partners and downstream function of *LZTR1* remain an open field of research (Nacak, Leptien, Fellner, Augustin, & Kroll, 2006). Others have proposed its role in RAS ubiquitination and resultant schwannoma progression using in vitro cellular models (Steklov et al., 2018). We performed a western blot analysis of heart tissue lysates to assess for signaling pathway phosphorylation levels using anti-phospho-ERK 1/2 and anti-phospho-AKT antibodies. Overt ERK 1/2 or AKT phosphorylation was not detected in any of the samples (Figure 3b). Immunohistochemical analysis of the adult heart and the vascular lesions also fell short of demonstrating clear differences in ERK 1/2 and AKT phosphorylation

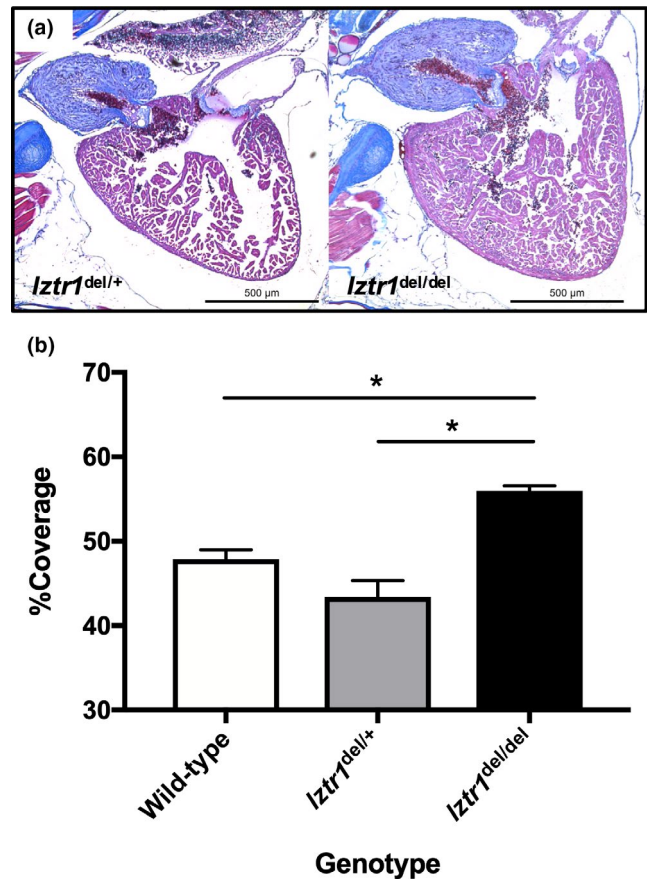


FIGURE 2 Biallelic functional loss of *lztr1* causes hypertrophy of the zebrafish heart. (a) Compared to control and $lztr1^{del/+}$ adult zebrafish, $lztr1^{del/del}$ homozygous mutants exhibit marked ventricular hypertrophy. (b) Quantitative comparison of the histology, by means of percent coverage of ventricular area by myocardial tissue, clearly depicts the prominent ventricular hypertrophy in $lztr1^{del/del}$ fish. Data are represented as the mean \pm SEM ($*p < .05$ vs. $lztr1^{del/+}$, two-tailed Welch's unpaired *t* test. $N = 3, 5, 5$ for wild-type, $lztr1^{del/+}$, $lztr1^{del/del}$, respectively)

levels (data not shown). These negative results were similar to the observation made in a zebrafish model of another RAS/MAPK syndrome, the Costello syndrome (Santoriello et al., 2009). We speculate that spatiotemporally regulated activation of these pathways may be escaping our analysis using adult zebrafish (Araki et al., 2004; Nakamura et al., 2007).

Autosomal-recessive NS is an emerging clinical entity to which our in vivo disease modeling experiments provide additive evidence on *LZTR1* pathogenicity. Judging from the fact that biallelic null variants have never been identified in mice or human patients, homozygous loss of *LZTR1* function must be causing embryonic lethality in both organisms (Johnston et al., 2018). Therefore, in vivo consequences of *LZTR1* deficiency had so far been assessed by the phenotypic observations from heterozygous $Lztr1^{del/+}$ mice. Such previous work, however, harbor some limitations; for example, incomplete recapitulation of the phenotype of human Noonan

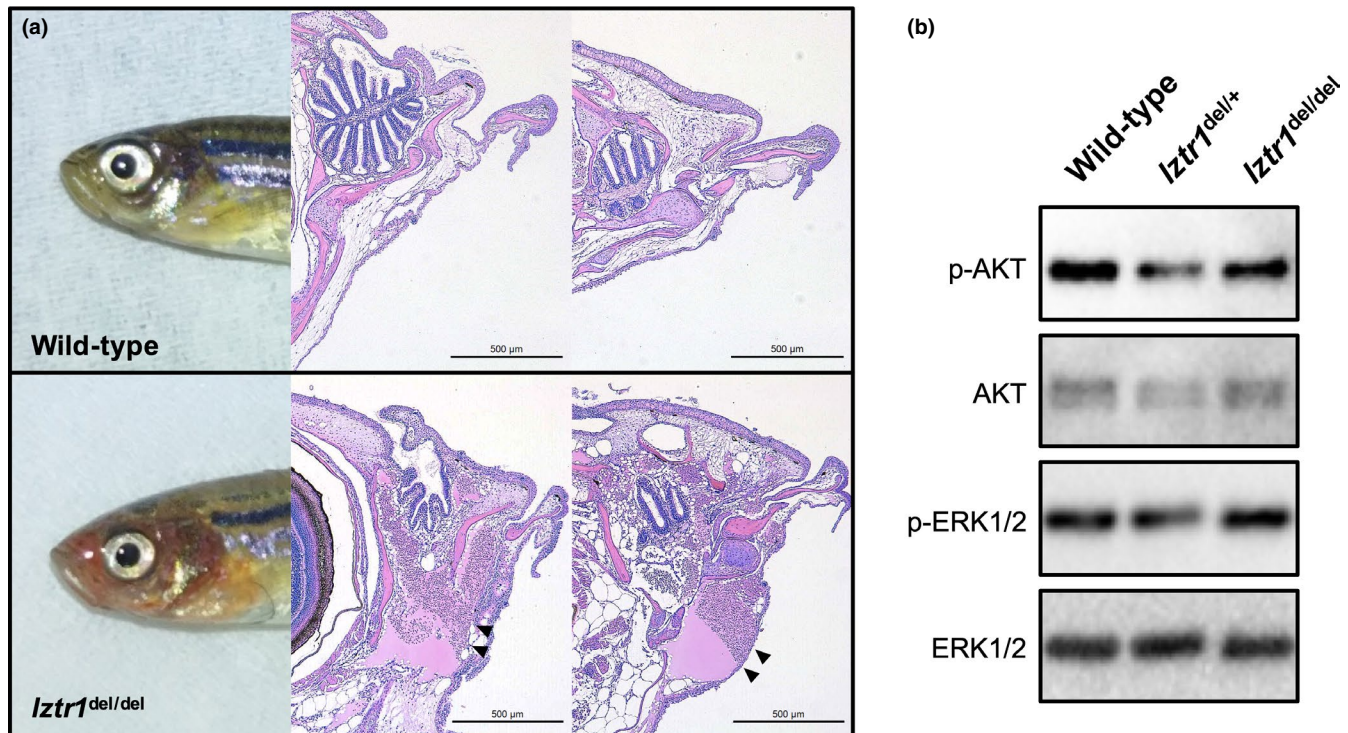


FIGURE 3 Analysis of extracardiac anomalies in *lztr1*^{del/del} mutants and the target signaling pathways downstream of *LZTR1*. (a) Vascular malformations could be observed in the *lztr1*^{del/del} mutants through the skin as a red coloration. Hematoxylin-eosin staining of longitudinal sections show the multiple vascular malformations (arrowheads) in the cranial part of the *lztr1*^{del/del} mutant. (b) Western blot analysis of heart lysates from control (wild-type and *lztr1*^{del/+}) and *lztr1*^{del/del} homozygous mutants detected with the indicated antibodies. No clear differences were obtained in signaling pathway phosphorylation levels

syndrome patients, who are more prone to concentric cardiac hypertrophy rather than the eccentric hypertrophy with increased diastolic dimensions seen in *Lztr1*^{del/+} mice (Steklov et al., 2018). We do admit that our zebrafish model harboring homozygous null variants does not perfectly mimic the human *LZTR1* mutational spectrum. We believe, however, that the form of myocardial hypertrophy seen in *lztr1*^{del/del} zebrafish closely resembles that of human disease, making the model suitable for analyzing especially the heart disease pathology. Since the zebrafish cardiomyocyte conveys advantages over the commonly used mouse cardiomyocyte in terms of feasible manipulation and culture (Sander, Suñe, Jopling, Morera, & Belmonte, 2013), we believe that our zebrafish model will

serve as a novel platform for pathophysiological investigation of RAS/MAPK syndrome-associated cardiomyopathy.

ACKNOWLEDGMENTS

R.I. received grants from Japan Society for the Promotion of Science KAKENHI (JP17J09192). Y.N. received research fellowships from Japan Society for the Promotion of Science, the Keizo Ohta Memorial Award 2018 from Morinaga Foundation for Health & Nutrition, and the Miyata Foundation Award for Young Scientists 2019. The authors have no conflict of interest to declare.

ORCID

Yu Nakagama  <https://orcid.org/0000-0001-9780-9719>

REFERENCES

- Abdul-Wajid, S., Demarest, B. L., & Yost, H. J. (2018). Loss of embryonic neural crest derived cardiomyocytes causes adult onset hypertrophic cardiomyopathy in zebrafish. *Nature Communications*, 9, 4603. <https://doi.org/10.1038/s41467-018-07054-8>
- Al-Olabi, L., Polubothu, S., Dowsett, K., Andrews, K. A., Stadnik, P., Joseph, A. P., Kinsler, V. A. Mosaic RAS/MAPK variants cause sporadic vascular malformations which respond to targeted therapy. (2018). *Journal of Clinical Investigation*, 128(4), 1496–1508. <https://doi.org/10.1172/JCI98589>

TABLE 2 Frequency of vascular malformations among different *lztr1* genotypes

Genotype	Frequency	%
<i>lztr1</i> ^{+/+}	0/8	0
<i>lztr1</i> ^{del/+}	0/8	0
<i>lztr1</i> ^{del/del}	8/8	100

Note: Vascular malformations, resembling human vascular pathology caused by RAS/MAPK activation, were observed exclusively in *lztr1*^{del/del} homozygous mutant zebrafish.

- Aoki, Y., Niihori, T., Inoue, S., & Matsubara, Y. (2016). Recent advances in RASopathies. *Journal of Human Genetics*, *61*, 33–39. <https://doi.org/10.1038/jhg.2015.114>
- Araki, T., Mohi, M. G., Ismat, F. A., Bronson, R. T., Williams, I. R., Kutok, J. L., ... Neel, B. G. (2004). Mouse model of Noonan syndrome reveals cell type- and gene dosage-dependent effects of *Ptpn11* mutation. *Nature Medicine*, *10*, 849–857. <https://doi.org/10.1038/nm1084>
- Jao, L. E., Wente, S. R., & Chen, W. (2013). Efficient multiplex bi-allelic zebrafish genome editing using a CRISPR nuclease system. *Proceedings of the National Academy of Sciences of the United States of America*, *110*, 13904–13909. <https://doi.org/10.1073/pnas.1308335110>
- Johnston, J. J., van der Smagt, J. J., Rosenfeld, J. A., Pagnamenta, A. T., Alswaid, A., Baker, E. H., ... Biesecker, L. G. (2018). Autosomal recessive Noonan syndrome associated with biallelic *LZTR1* variants. *Genetics in Medicine*, *20*, 1175–1185. <https://doi.org/10.1038/gim.2017.249>
- Nacak, T. G., Leptien, K., Fellner, D., Augustin, H. G., & Kroll, J. (2006). The BTB-kelch protein *LZTR-1* is a novel Golgi protein that is degraded upon induction of apoptosis. *The Journal of Biological Chemistry*, *281*, 5065–5071. <https://doi.org/10.1074/jbc.M509073200>
- Nakaguma, M., Jorge, A. A. L., & Arnhold, I. J. P. (2019). Noonan syndrome associated with growth hormone deficiency with bi-allelic *LZTR1* variants. *Genetics in Medicine*, *21*, 260. <https://doi.org/10.1038/s41436-018-0041-5>
- Nakamura, T., Colbert, M., Krenz, M., Molkentin, J. D., Hahn, H. S., Dorn, G. W. 2nd, & Robbins, J. (2007). Mediating ERK 1/2 signaling rescues congenital heart defects in a mouse model of Noonan syndrome. *The Journal of Clinical Investigation*, *117*, 2123–2132. <https://doi.org/10.1172/JCI30756>
- Richards, S., Aziz, N., Bale, S., Bick, D., Das, S., Gastier-Foster, J., ... Rehm, H. L. (2015). Standards and guidelines for the interpretation of sequence variants: A joint consensus recommendation of the American College of Medical Genetics and Genomics and the Association for Molecular Pathology. *Genetics in Medicine*, *17*, 405–424. <https://doi.org/10.1038/gim.2015.30>
- Sander, V., Suñe, G., Jopling, C., Morera, C., & Belmonte, J. C. I. (2013). Isolation and in vitro culture of primary cardiomyocytes from adult zebrafish hearts. *Nature Protocols*, *8*, 800–809. <https://doi.org/10.1038/nprot.2013.041>
- Santoriello, C., Deflorian, G., Pezzimenti, F., Kawakami, K., Lanfrancione, L., d'Adda di Fagagna, F., & Mione, M. (2009). Expression of H-RASV12 in a zebrafish model of Costello syndrome causes cellular senescence in adult proliferating cells. *Disease Models & Mechanisms*, *2*, 56–67. <https://doi.org/10.1242/dmm.001016>
- Steklov, M., Pandolfi, S., Baietti, M. F., Batiuk, A., Carai, P., Najm, P., ... Sablina, A. A. (2018). Mutations in *LZTR1* drive human disease by dysregulating RAS ubiquitination. *Science*, *362*, 1177–1182. <https://doi.org/10.1126/science.aap7607>
- Umeki, I., Niihori, T., Abe, T., Kanno, S.-I., Okamoto, N., Mizuno, S., ... Aoki, Y. (2018). Delineation of *LZTR1* mutation-positive patients with Noonan syndrome and identification of *LZTR1* binding to RAF1–PPP1CB complexes. *Human Genetics*, *138*, 21–35. <https://doi.org/10.1007/s00439-018-1951-7>
- Zhu, X., Xu, Y., Yu, S., Lu, L. U., Ding, M., Cheng, J., ... Tian, Y. (2014). An efficient genotyping method for genome-modified animals and human cells generated with CRISPR/Cas9 system. *Scientific Reports*, *4*, 6420. <https://doi.org/10.1038/srep06420>

How to cite this article: Nakagama Y, Takeda N, Ogawa S, et al. Noonan syndrome-associated biallelic *LZTR1* mutations cause cardiac hypertrophy and vascular malformations in zebrafish. *Mol Genet Genomic Med*. 2020;8:e1107. <https://doi.org/10.1002/mgg3.1107>